

Measuring the isotope effect on the gross Beryllium erosion in JET

E. de la Cal¹, D. Borodin², I. Borodkina², D. Douai³, E. Pawelec⁴, A. Shaw⁵, S. Silburn⁵, I. Balboa⁵, S. Brezinsek², P. Carvalho⁵, T. Dittmar², A. Huber², V. Huber², J. Karhunen⁶, U. Losada¹, A. Manzanares¹, J. Romazanov², A. Tookey⁵, and JET contributors^{*}

¹ Laboratorio Nacional de Fusión, CIEMAT, Av. Complutense 40, E-28040 Madrid, Spain

² Forschungszentrum Jülich GmbH, Institut für Energie- und Klimaforschung-Plasmaphysik, D-52425, Jülich, Germany

³ CEA, IRFM, F-13108 Saint-Paul-lez-Durance, France

⁴ University of Opole, Institute of Physics, Oleska 48, Opole, Poland

⁵ CCFE Fusion Assoc., Culham Science Centre, Abingdon, OX14 3DB, UK

⁶ Aalto University, Department of Applied Physics, 02150 Espoo, Finland

^{*} See the author list of ‘Overview of JET results for optimising ITER operation’ by J. Mailloux et al. to be published in Nuclear Fusion Special issue: Overview and Summary Papers from the 28th Fusion Energy Conference (Nice, France, 10-15 May 2021)

e-mail: e.delacal@ciemat.es

Abstract

The isotope effect, hydrogen (H) versus deuterium (D), on the gross Beryllium (Be) erosion yield has been measured in Ohmic limiter plasmas in JET tokamak by spectroscopic means. A simplified method to extract the effective sputtering yield from the quotient of the radiances of the D_α or D_γ and the Be II lines at 527.1 nm was applied. A clear isotope effect has been found, the erosion yield of D being about a factor of 2 larger compared to H in the whole explored plasma density range. This is in agreement with physical sputtering data obtained with H^+ and D^+ ion beams and also with material surface computer simulations. The already published contribution of chemically assisted physical sputtering (CAPS) has been also identified here. Currently the study is being extended to tritium (T) and D-T plasmas and the effect of helium mixtures.

1. Introduction

JET, with its ITER-like metallic wall (ILW) is provided with Be limiters that protect the inner and outer first wall and a W divertor [see e.g. 1]. A recent review of the latest results for optimising ITER operation including first results of latest fuel isotope can be found in [2]. JET is the only fusion device operating with Be and thereby the sole where its erosion can be studied in situ and moreover, with a similar reactor geometry, magnetic topology and edge plasma conditions as ITER. Due to the much longer duty cycle compared with today’s fusion devices, extrapolation from actual experimental studies try to anticipate in how much the lifetime of ITER’s PFCs will be limited by plasma erosion [see e.g. 3-7], but experimental observations to validate these models remain scarce. Besides the erosion problem of the Be components, a major concern is the formation of co-deposits due to the sputtered, transported and re-deposited Be

atoms that will be the dominant tritium (T) retention mechanism [see e.g. 8-10]. Additionally, Be will be the dominant intrinsic impurity in ITER plasmas arriving to the tungsten (W) divertor increasing its erosion and its concentration in the confined plasma thereby affecting negatively the reactor's global performance [see e.g. 11-13].

Dedicated erosion experiments were done in the past in JET where the plasma and Be fluxes were measured using spectroscopic means. In [14-16] the so-called Be effective sputtering yield $Y_{\text{Be}}^{\text{eff}}$ (see later) was studied using a plasma density scan to vary the impact energies of impinging deuterium ions. Additionally in [15] the physical and chemical branches of the Be sputtering yields were determined. These data were used for interpreting Be migration studies including post mortem-analysis [17-18] and to validate the results obtained with the impurity transport code ERO [16, 19]. A recent review including also basic laboratory experiments and computer simulations about Be erosion and fuel retention can be found in [10]. Despite the importance of the possible isotope effect on the erosion yield, no dedicated in-situ experimental studies on this topic have been done or at least published and the bibliography is relatively sparse showing generally a large dispersion in the data. In a paper of 1997 [20] a summary was given on data of physical sputtering yields Y_{Be} of H, D, T and other atoms on Be collected from laboratory experiments with ion beams and also on computer simulations. Unfortunately, the dispersion of the collected data is quite large, especially for ion impact energies $E_i < 100$ eV. The general trend is however that for normal incidence, H and D show similar dependency of Y_{Be} on the ion energy in the range of $10 \text{ eV} < E_i < 1 \text{ keV}$, but the absolute values are approximately a factor of 2 larger for D due to the mass effect. Other aspects such as the effect of the ion incident angle or the yields of impurity species as helium, carbon and oxygen and Be itself are also described. In a recent publication [21] a similar isotope mass dependence on $Y_{\text{Be}}^{\text{eff}}(E_i)$ is proposed, but with higher absolute values by a factor of about 2 for all isotopes.

In the present work we experimentally investigate the isotope effect, H versus D, on the gross Beryllium erosion at the JET limiters taking advantage of the recent dedicated isotope campaigns [2]. We begin firstly by describing the plasmas here analysed, as well as the main diagnostics and also the way the erosion yield $Y_{\text{Be}}^{\text{eff}}$ is inferred. Then, examples are shown of similar plasmas in H and D where the Be fluxes are compared and an extensive database is analysed. A clear isotope effect on $Y_{\text{Be}}^{\text{eff}}$ is found. Finally the results are discussed in view of the bibliography mentioned before.

2. Experiment description and $Y_{\text{Be}}^{\text{eff}}$ estimation

In the first part of this work, Ohmic limiter plasmas from dedicated Be-erosion experiments in H and D are analysed. Discharges (toroidal magnetic field $B_T = 2.3$ T and plasma current $I_p = 1.9$ MA) of up to 20 s duration and more to heat up the inner limiters including plasma density scans with $\langle n_e \rangle$ of $1.5 - 4 \times 10^{19} \text{ m}^{-3}$ were performed repetitively along two consecutive half-day shifts. The limiter heating was done to study the effect of the limiter surface temperature on the Chemical Assisted Physical Sputtering (CAPS) and the density scan to vary the edge plasma T_e and thereby the impinging ion energy on the limiters [15]. Later, so-called "Limiter-cycling" discharges ($B_T = 2.3$ T and $I_p = 1.8$ MA) are analysed where the Strike Point (SP) of the plasma Separatrix rotates several times around the inner and outer limiters. These kinds of discharges are used in JET for conditioning of the first wall, i.e for impurity cleaning or for fuel isotope control. The goal of studying these plasmas was to extend the database and also to compare the yields at the inner and outer limiters as obtained with the wide-angle view cameras.

The principal two diagnostics measure the plasma photon fluxes directed to the limiters and those of the sputtered Be. The first is the spectroscopy system also used for the same issue in the past [14-16] that collects horizontally light from a spot at the border of a limiter at the near

SOL close to the inner mid-plane. The light is transported to a spectrometer system and different atomic lines such as the here used $D_\gamma/(H_\gamma)$ and Be II (527.1 nm) are routinely acquired with a time resolution of 100 ms. The second are two wide-angle view visible cameras installed outside the JET biological shield that receive the image from an equatorial port after being transported along a path of more than 10 m. One is equipped with a filter centred at the Be II 527 nm line and the other is an unfiltered High-speed or Fast camera but where the light was demonstrated to be clearly dominated by D_α (H_α) atomic emission [22]. Both cameras were recently calibrated and the measurements at the same limiter location where the spectrometer looks at are in good agreement [*].

The Be effective sputtering yield Y_{Be}^{eff} (or simply Y^{eff}) is defined as:

$$(1) \quad Y_{Be}^{eff} \equiv \frac{F_{Be}^{out}}{F_D^{in}}$$

where F_{Be}^{out} is the Be out-flux sputtered from the surface by the bombarding plasma in-flux F_D^{in} (D stays here for deuterium meaning also H in the case of a hydrogen plasma). The Be out-flux has two sputtering precursors from the plasma, the majority impinging D flux (the fuel) and the impurity flux, mainly Be in JET, that causes the so-called self-sputtering. In fact, equation (1) can be rewritten as [14]:

$$(2) \quad Y_{Be}^{eff} = \frac{Y_{Be>D}}{1 - xY_{Be>Be}}$$

where $Y_{Be>D}$ is the Be sputtering yield due to D, $Y_{Be>Be}$ is the self-sputtering yield and x is the Be fraction returning onto the surface. The major contribution of $Y_{Be>D}$ is physical sputtering, the other being CAPS, that mainly produces the volatile molecule BeD. CAPS has been measured in JET to contribute up to 30% for the base operational limiter temperature of $T \approx 200$ °C and decreases as the surface temperature increases, vanishing for $T > 500$ °C [15]. In the present work the global yield is measured without distinguishing between both mechanisms.

On the other hand, we can retrieve for a specie A its particle flux F_A entering a plasma by spectroscopic means from the measurement of a characteristic line radiance $L_{\lambda A}$ using the “so-called” S/XB photon efficiencies [23] and equation (1) can be rewritten as:

$$(3) \quad Y_{Be}^{eff} = \frac{(S/XB)_{\lambda Be} L_{Be}}{(S/XB)_{\lambda D} L_D} \approx 1.8 \frac{L_{Be}}{L_D}$$

The S/XB coefficients depend on the plasma electron density n_e and temperature T_e and can be retrieved for many characteristic atomic lines from the ADAS database [24]. Unfortunately significant uncertainties appear when applying the S/XB-method due to different reasons and approximations must be taken. In most cases, the main uncertainty comes from the fact that the radiance is a line-integrated measurement along the plasma edge emission layer and therefore a mean S/XB must be estimated since generally the n_e -, the T_e - and the emission-radial profiles are unknown. Here, we take advantage of the fact that the ratio of the S/XB coefficients of the measured atomic lines, Be II at 527 nm and D_α (H_α) or D_γ (H_γ), have a relatively small dependence near the Separatrix on n_e and T_e for the limiter plasmas analysed here and we fix this ratio to a constant equal to 1.8 [*]. When making this approximation we accept an error in the calculation that is estimated to be $< \pm 50\%$, not much larger than generally assumed for this kind of measurements. However, this error should be much smaller when comparing the relative values of the yields for H and D, since equivalent discharges, that should have similar edge plasma parameters, have been compared.

3. Results

The upper frames of **figure 1** show the time traces of the average electron density $\langle n_e \rangle$ for a D (a) and a similar H (b) Ohmic plasma leaning at the inner limiters. The discharges pertain to the dedicated Be-erosion experiments described in the last section. A video of a typical density ramp limiter plasma ending with a Marfe can be seen clicking [here](#) (see also link below)¹. In the lower frames are displayed the radiances L of the D_γ/H_γ (blue) and Be II (red) atomic lines measured by the spectrometer looking at the inner limiter mid-plane throughout the density ramp-ups. As expected, they increase monotonically with $\langle n_e \rangle$, till the plasma is displaced towards the outer limiters (yellow stripes). The D_γ/H_γ radiances show similar values for equivalent $\langle n_e \rangle$ in both H and D plasmas indicating similar plasma fluxes to the limiters as expected. However the Be II emission is about two times larger for the D plasma compared to the H one. When calculating Y^{eff} using equation (3) with $L_{H\alpha} \approx 30 L_{H\gamma}$ (see e.g. [14]) we get the time traces (green) shown in the same figures. For the D plasma, $0.15 < Y^{\text{eff}} < 0.2$, whereas for the H plasma the value range is about the half. The same trend is observed with the cameras. In **figure 2** a) and b) we show for the same plasmas in the upper frames the images recorded with the Be II camera inner limiters for the above described D and H plasmas. Both were taken with the same camera settings at the time instants marked with a dashed line in **figure 1** where $\langle n_e \rangle \approx 3 \times 10^{19} \text{ m}^{-3}$ for both plasmas. The white circle shows approximately the spot where the spectrometer is looking at. It can be depicted from the false colour scale that the Be II emission intensity is a factor of about 2 stronger for the D plasma. Using the calibration factors the radiances at the limiter marked with a dashed rectangle can be retrieved from the camera intensities. In the lower frames are displayed the time traces corresponding to the same time intervals as in **figure 1** of the maximum radiance values at the marked limiter. For the D plasma only the Be II filtered camera was operative, but for the H plasma, in addition the unfiltered Fast camera was recording data so that the H_α -radiance from which the one of H_γ - can be estimated. Looking first to the Be II radiances (red traces) it can be seen that they have a similar time behaviour as the corresponding of **figure 1**. Again, about 2 times higher values are obtained for the D compared to the H plasma. Note however that the absolute camera values are approximately a factor of 4 higher compared to the spectrometer ones. This is due to the fact that, while the camera data here shown correspond to the maximum value of the whole limiter surface, those of the spectrometer are an average of a fixed spot localised between the limiter corner and the wall where the emission is expected to be much smaller. For the case of the H plasma, where also the H_γ -radiance was estimated (blue trace), the relative value respect the Be II one is similar to those of figure 1 and therefore also the Y^{eff} (green) estimated from the camera emission intensities.

The extensive database of the dedicated Be-erosion experiments in D and H was analysed in a similar way as shown above. The spectrometer data of totally 60 plasma periods of 20 similar Ohmic limiter plasmas in H and D were selected for different densities. Attention was paid to choose only the time periods when the plasma was striking at the mid-plane of the limiter where the spectrometer was looking at because this position affects the measured photon fluxes. **Figure 3** shows the atomic line radiances L of the a) D_γ/H_γ and b) Be II as a function of the average electron line density $\langle n_l \rangle$ ($\approx 2.2 \text{ m} \langle n_e \rangle$) for the analysed D (red) and H (blue) plasmas. Again we observe that, whereas the D_γ/H_γ show similar values, those of Be II are about two times larger for the D plasma compared to the H for same densities. In **figure 4** a) is displayed for the same

¹ http://www-fusion.ciemat.es/fileshare/doc_exchange/JET%202021%20deCal/ne_ramp.mp4

data the calculated Y^{eff} , that if fitted to constant values (dashed lines), give for D a mean value of $Y^{\text{eff}}_{\text{Be>D}} \approx 0.18$, and for H about the half, $Y^{\text{eff}}_{\text{Be>H}} \approx 0.085$. The dispersion is relatively small, less than +/- 15%, except for the points marked within the ellipses and the rectangle only in the D plasmas at the highest densities (these points were not taken into account for the mean value calculation). The points within the rectangle were in fact close to the density limit where the plasma edge cools down and radiative instabilities called “MARFES” begin to develop. In these conditions it is to be expected that the sputtering strongly falls due to the E_i decrease. The reason of the low Y^{eff} values encircled with the ellipses at lower densities may be attributed to the gradual inhibition of CAPS with the increasing limiter temperature. In the past it was observed, that the CAPS contribution of about 30% to the total Y^{eff} begins to fall when the limiter surface temperature $T_{\text{surf}} > 300$ °C and is completely inhibited for $T_{\text{surf}} > 500$ °C [15]. **Figure 4 b)** shows the same data as those of **figure 4 a)** but represented against T_{surf} at the mid-plane as measured by thermography. A similar trend as in [15] is observed here for H. For D however, we see above 300 °C first a Y^{eff} decrease till about 500 °C, but unexpectedly the yield increases then for higher temperatures. To better investigate the CAPS contribution, we analysed the evolution of the band emission of the BeD (BeH) molecule at 496.0–499.4 nm, which is monitored routinely with the same spectroscopy system and view. In **figure 4c)** is represented for the same plasmas the ratio of the BeD (BeH) to D_γ (H_γ) radiances as a function of T_{surf} . In agreement with [15, recent reference?], this ratio and therefore the CAPS erosion decreases with T_{surf} in a similar monotonical way for both, D and H plasmas. This means that the Y^{eff} increase for the analysed D plasmas for $T_{\text{surf}} > 500$ °C remains unclear and further analysis is necessary.

Finally, **figure 5** shows the Z_{eff} for the same plasma periods as a function of $\langle n_{\text{le}} \rangle$ for D and H (the measurements were not available for all points). The expected decrease of Z_{eff} with the density is clear in both. However, the absolute values are sensibly larger for D compared to H plasmas for similar densities, something to be linked to the higher Be concentration because of the higher Y^{eff} and thereby higher Be fluxes in the D plasmas.

The other analysed plasma types are the so-called “Limiter-cycling” discharges used in JET for wall conditioning where the plasma contacts all limiter surfaces of the vacuum vessel. A video of one cycling period can be seen clicking [here](#) (see also link below)². **Figure 6** shows the time traces of the line averaged density $\langle n_{\text{le}} \rangle$, the radiances L of the D_γ/H_γ and Be II lines and of the calculated Y^{eff} for a H (blue) and a D (red) “Limiter-cycling” discharge. The yellow stripes mark the periods when the plasmas were leaning at the inner limiters. Note that there $\langle n_{\text{le}} \rangle$ decreases and the emission intensities D_γ/H_γ and Be II monitored by the spectrometer strongly increase. It is to be noted that L_{D_γ/H_γ} depends on the vertical position of the plasma SP along the limiter and also on $\langle n_{\text{le}} \rangle$. Thanks to the cameras, the spatial emission distribution can be visualised and the SP position identified and Y^{eff} (lowest frame) is shown only when the plasma was at or close to the mid-plane where the spectrometer is looking at. Again we can see that Y^{eff} is for D always sensibly higher than for H. Interestingly, we get for H a very similar yield range $0.08 < Y^{\text{eff}}_{\text{Be>H}} < 0.1$ and for D $0.18 < Y^{\text{eff}}_{\text{Be>H}} < 0.3$, the upper range reaching higher values here (see later). **Figure 7a** shows for the same plasmas the emission images captured by the Be II filtered camera at the instant marked in **figure 6** with a vertical line and where $\langle n_{\text{le}} \rangle$ and also L_{D_γ/H_γ} were similar in both. The intensities were corrected for the different exposure times. The arrows mark the mean values of the marked region near the mid-plane and the approximate observation spot of the spectrometer with a circle. In accordance with the spectrometer data, the

² http://www-fusion.ciemat.es/fileshare/doc_exchange/JET%202021%20delaCal/Limiter_Cycling.mp4

Be II emission intensity is for D approximately two times stronger than for H. Thanks to the wide-angle view of the cameras also the outer limiters can be observed and a similar isotope effect is found systematically. This is shown in **Figure 7b** from another pair of “Limiter-cycling” plasmas in D and H where the camera settings were the same for both. The images were taken at the same plasma magnetic configuration and similar densities in both. Once more, the Be II emission intensity averaged over one of the observed outer limiters is for the D plasma twice that of the H one. To finalise, we display in **figure 8** the yields Y^{eff} as a function of $\langle n_l \rangle$ for the today collected “Limiter Cycling “ plasmas in D and H. The solid points are obtained from spectrometer measurements, the hollow from the cameras. The dashed lines mark the yields obtained for the dedicated erosion experiments at higher densities and the circles the plasmas of **figure 6**. In accordance with previous studies [14, 15], at the lowest densities $Y^{\text{eff}}_{\text{Be}}$ increases, at least this is clear for D. This was attributed to an increase in the Be self-sputtering contribution. Unfortunately, data at high density for D and at low density for H are scarce or missing. The idea is to extend this database and include also similar discharges from the actual T and D-T campaigns.

4. Summary and discussion

In this work we have measured by spectroscopic means the isotope effect, hydrogen (H) versus deuterium (D), on the Be effective sputtering yield $Y^{\text{eff}}_{\text{Be}}$ in Ohmic limiter plasmas in JET tokamak. The analysis is performed using the data collected by a dedicated spectrometer system looking to the mid-plane of an inner limiter and by two wide-angle view cameras with a global view of the reactor chamber including also the outer limiters. A simplified method to extract the effective sputtering yield from the quotient of the measured radiances of the D_α or D_γ and the Be II lines at 527 nm was applied. Since equivalent plasmas with similar edge parameters as n_e and T_e in H and D were compared, the relative error on the isotope effect of the estimated $Y^{\text{eff}}_{\text{Be}}$ values should be small. A large database of dedicated Ohmic limiter plasmas in separated H and D campaigns was analysed and a clear mass effect was found (see **figure 4**). The Be erosion yield of D is about a factor of 2 larger compared to H in the whole explored plasma density range. This result is in agreement with physical sputtering data obtained in laboratories with H^+ and D^+ ion beams and also with material surface computer simulations. The already documented contribution of CAPS has been also identified. As already shown [15, new reference?], its relative contribution to $Y^{\text{eff}}_{\text{Be}}$, is of about 30% for D and nearly 50% for H for surface temperatures < 300 °C and decreases monotonically as the temperature becomes higher. This was clearly seen for H, but for the analysed D plasmas at the highest temperatures (> 500 °C) unexpectedly high $Y^{\text{eff}}_{\text{Be}}$, were obtained. The reason for this is unclear and further analysis is necessary. Consistently with the reported isotope effect on the Be erosion yield, it has been found that the Z_{eff} of the D studied limiter plasmas is systematically larger compared to H ones (**figure 5**).

In addition to the dedicated erosion limiter experiments in H and D, so-called “Limiter-cycling” plasmas were also analysed. These discharges are used in JET whenever necessary in any kind of experiment for conditioning of the first wall, i.e for impurity cleaning or for fuel isotope control. Since these plasmas have outer and inner limiter configuration, they offer a continuously running collection of plasmas for Be erosion studies as the present one. In fact here it is shown that the analysed plasmas confirm the previous result, namely the clearly higher $Y^{\text{eff}}_{\text{Be}}$ for D compared to H, also at the outer limiters. The idea is to extend this database and include also similar discharges from the actual and coming T and D-T campaigns.

Concerning the absolute values of the obtained yield, it is in the same range and in accordance with previous results from JET [14-16]. Its strong increase for $\langle n_e \rangle < 1.5 \times 10^{19} \text{ m}^{-3}$ has been also observed for D, although not so clearly for H. However, the estimated $Y^{\text{eff}}_{\text{Be}}$ values

are constant for the rest of the plasma density regimes in contrast with the prior studies. This can be at least partly attributed to the here-assumed constant S/XB ratio (equation 3), since this quotient is expected to increase as the n_e increases and T_e falls.

Future work will focus on following items:

- Extend the Y_{Be}^{eff} database to T and D-T limiter plasmas and study the effect of helium mixtures.
- Improve the simplified S/XB method including edge n_e and T_e estimations for different plasma density conditions. Validation with plasma edge transport codes would be therefore valuable.
- Analyse plasmas with divertor configuration including L- and H-mode, resolving if possible inter- and intra-ELM periods and study the effect of ICRH and NBI heating on the yield. Also, try to identify if the isotope effect on the Be erosion influences the W divertor sputtering.

Acknowledgements

This work has been carried out within the framework of the EUROfusion Consortium, funded by the European Union via the Euratom Research and Training Programme (Grant Agreement No 101052200 - EUROfusion). Views and opinions expressed are however those of the author(s) only and do not necessarily reflect those of the European Union or the European Commission. Neither the European Union nor the European Commission can be held responsible for them.

5. References

- [1] G F Matthews et al 2013 J. Nucl. Mater. 438 S2
- [2] J Mailloux J. 2022 Nucl. Fusion in press <https://doi.org/10.1088/1741-4326/ac47b4>
- [3] S Carpentier et al 2011 J. Nucl. Mater. 415 S165
- [4] D Borodin et al 2011 Phys. Scr. T145 14008
- [5] D Borodin et al 2019 Nucl. Mat. and Energy 19 510
- [6] A Kirschner et al 2015 J. Nucl. Mat. 463 116
- [7] J Romazanov et al 2021 Nucl. Mat. and Energy 26 100904
- [8] K Schmid et al 2015 J. Nucl. Mat. 463 66
- [9] A Khan et al Nuclear Materials and Energy 20 (2019) 1006742
- [10] G De Temmerman 2021 Nuclear Materials and Energy 27 100994
- [11] N Den Harder 2016 Nucl. Fusion 56 026014
- [12] A Kirschner et al 2019 Nucl. Mat. and Energy 18 239
- [13] A Huber et al 2019 Nucl. Mat. and Energy 18 118
- [14] M Stamp et al 2010 J. Nucl. Mat. 415 S170
- [15] S Brezinsek et al 2014 Nucl. Fusion 54 103001
- [16] D Borodin et al 2014 Phys. Scr. T 159 014057
- [17] S Brezinsek et al 2015 Nucl. Fusion 55 063021
- [18] A Widdowson et al 2014 Phys. Scr. T 159 014010
- [19] J Romazanov et al 2019 Nucl. Mat. and Energy 18 331
- [20] J Roth et al 1997 Fus. Eng. Des. 37 465
- [21] P Yu Babenko et al 2020 Plasma Phys. Control. Fusion 62 045020
- [22] E de la Cal et al 2020 Plasma Phys. Control. Fusion 62 035006
- [*] E de la Cal et al, sent for publication
- [23] K H Behringer et al, PPCF 31 (1989) 2059
- [24] ADAS, <http://adas.phys.strath.ac.uk>

Figure 1: The upper frames show the densities $\langle n_e \rangle$ for a D (a) and a similar H plasma (b). Below are displayed the radiances L of the D_γ/H_γ (blue) and Be II (red) lines measured by the spectrometer and the calculated yields Y^{eff} (green).

Figure 1

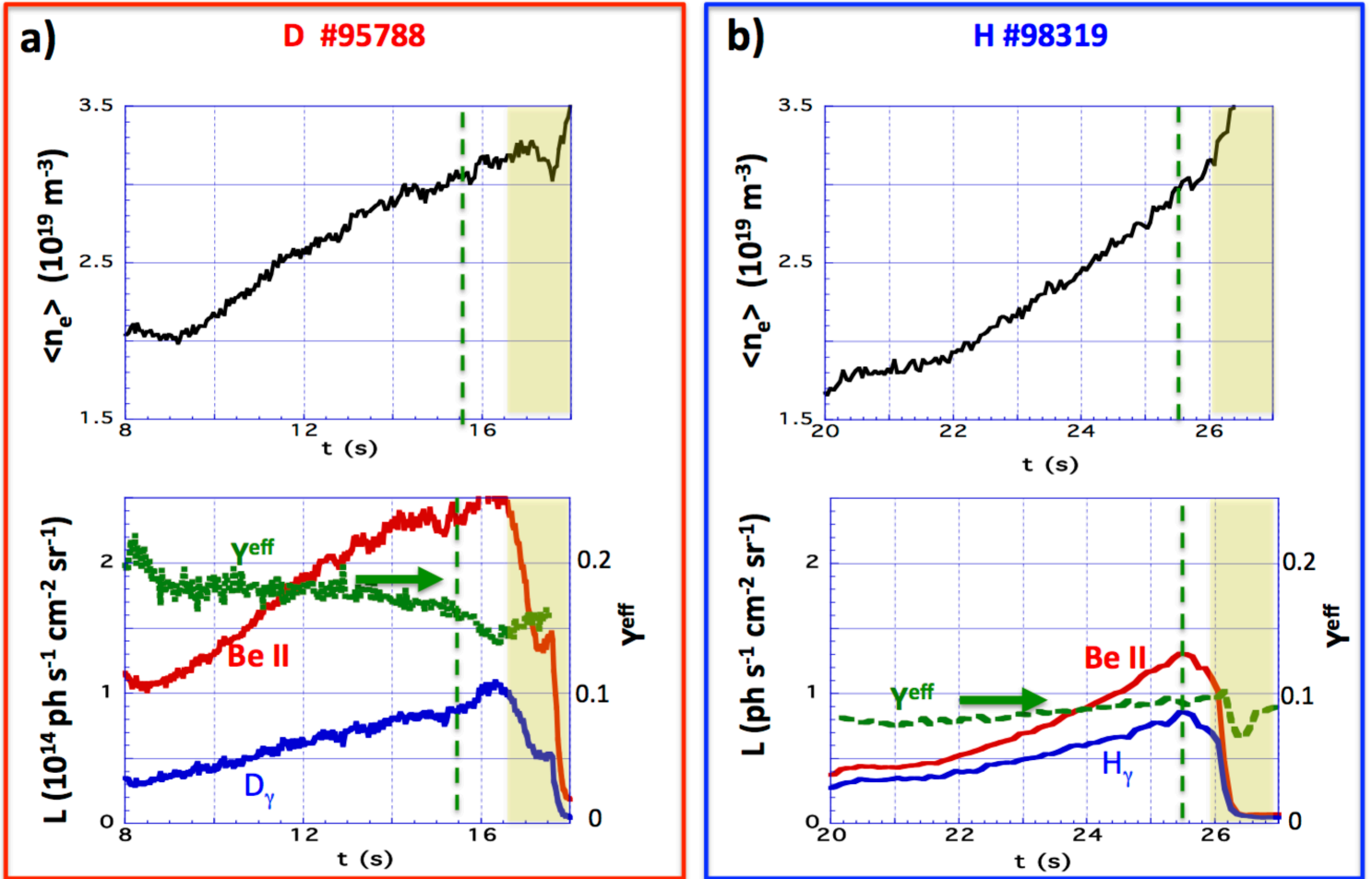


Figure 2: Images of the observed inner limiters recorded with the Be II camera for the same plasma as in figure 1 (see text). Below are shown the radiances L of the H_γ (blue) and Be II (red) lines measured by the cameras and Y^{eff} (green).

Figure 2

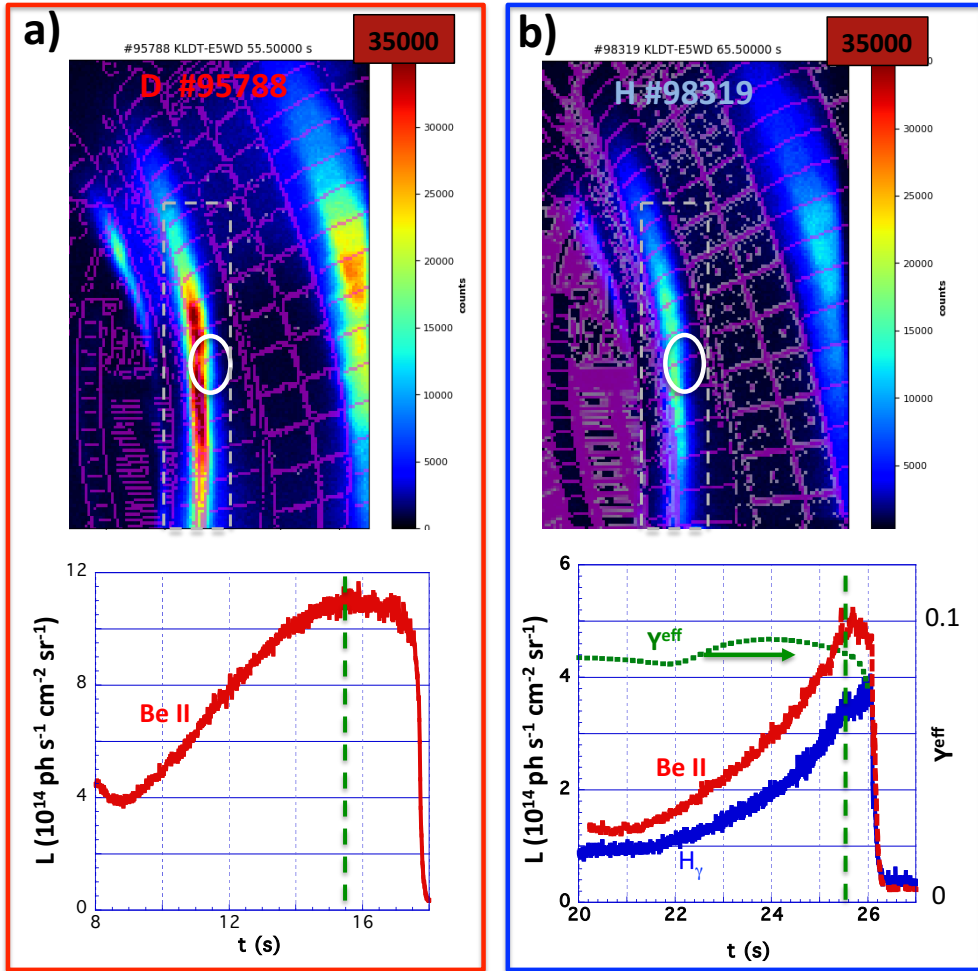


Figure 3: Radiances L of the a) D_γ/H_γ and b) Be II lines as a function of the averaged line density $\langle nl_e \rangle$ ($\approx 2.2 \text{ m} \langle n_e \rangle$) for all the analysed D (red) and H (blue) plasmas of the Be erosion experiments.

Figure 3

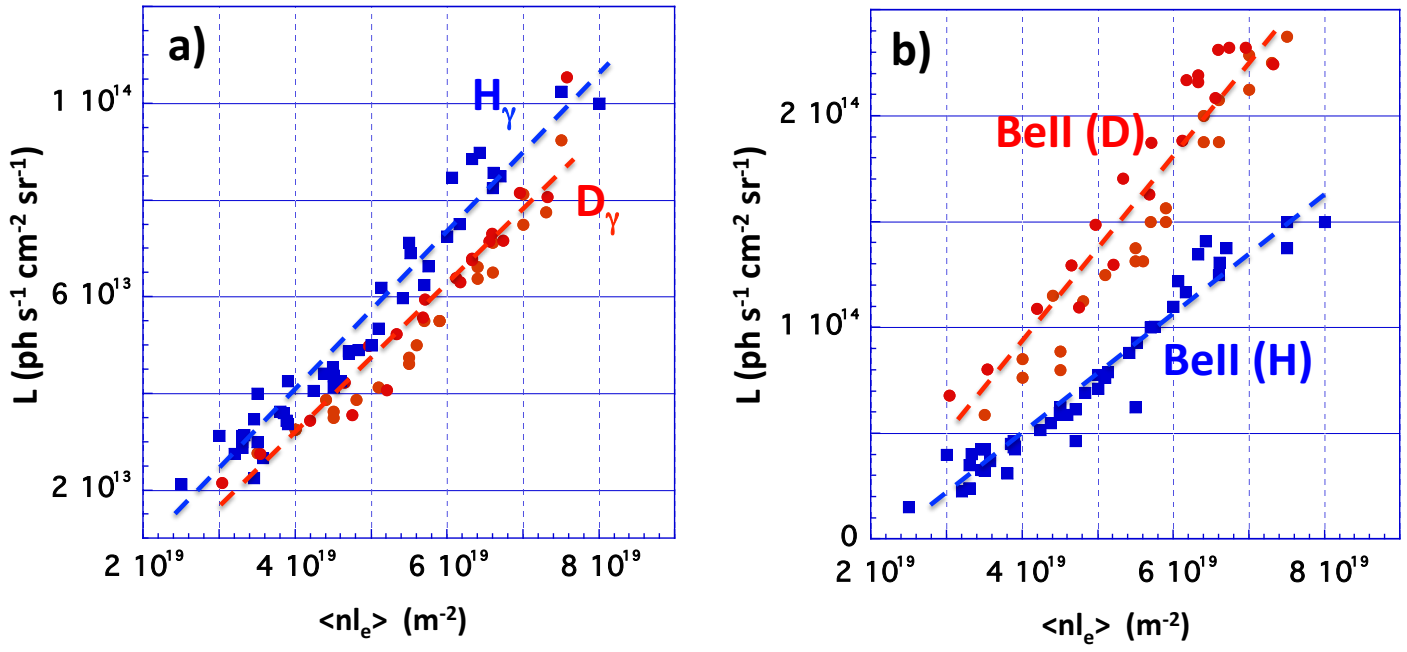


Figure 4: a) Calculated γ^{eff} values as a function of $\langle n l_e \rangle$ for D (red) and for H (blue) obtained from the data of figure 3. b) Same yields but represented as a function the measured surface limiter temperature T_{surf} at the limiter mid-plane. c) Ratio of BeD (BeH) to D_γ (H_γ) radiances as a function of T_{surf} .

Figure 4

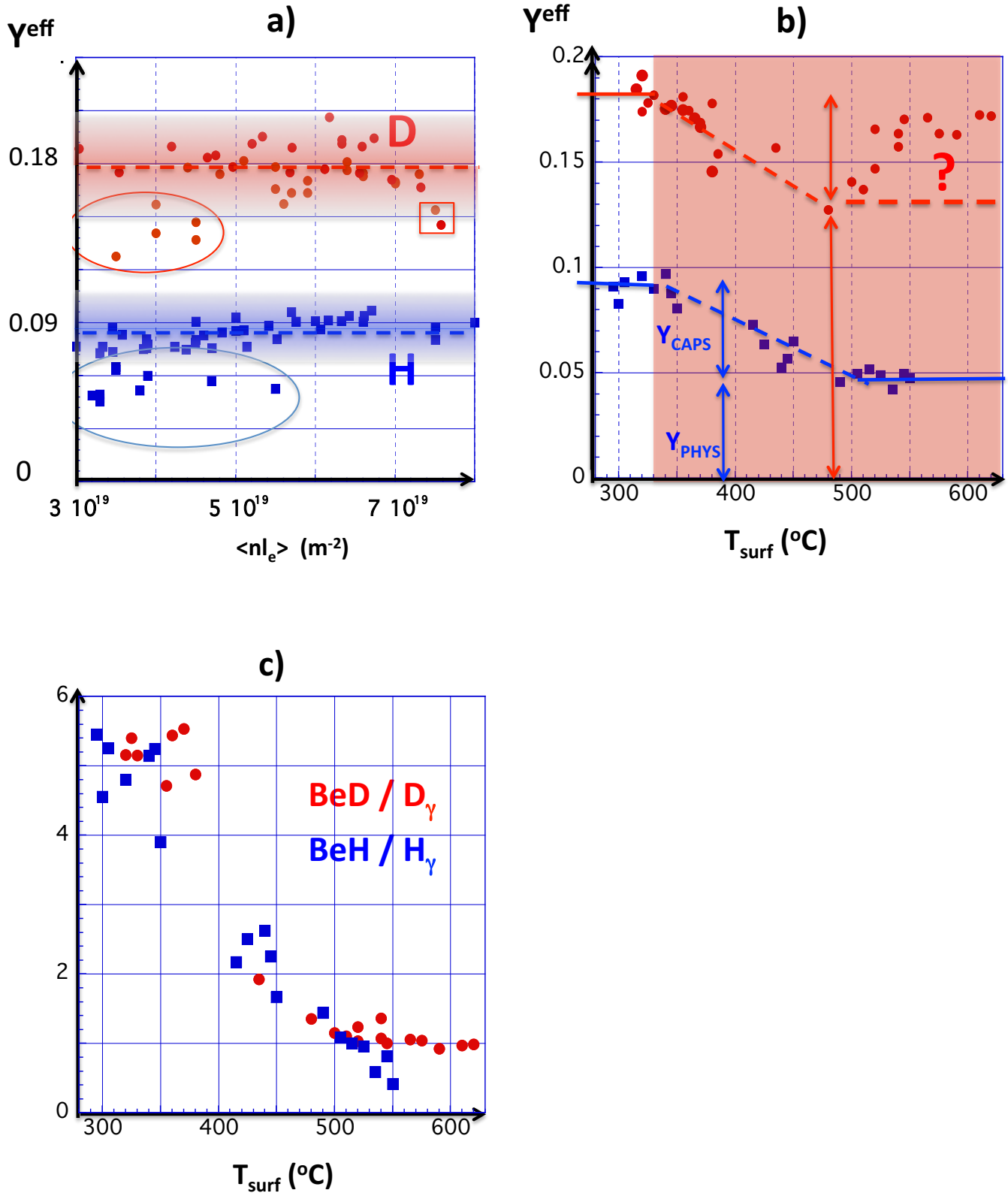


Figure 5: Z_{eff} for the analysed plasma periods as a function of $\langle n l_e \rangle$ for D (red) and H (blue)

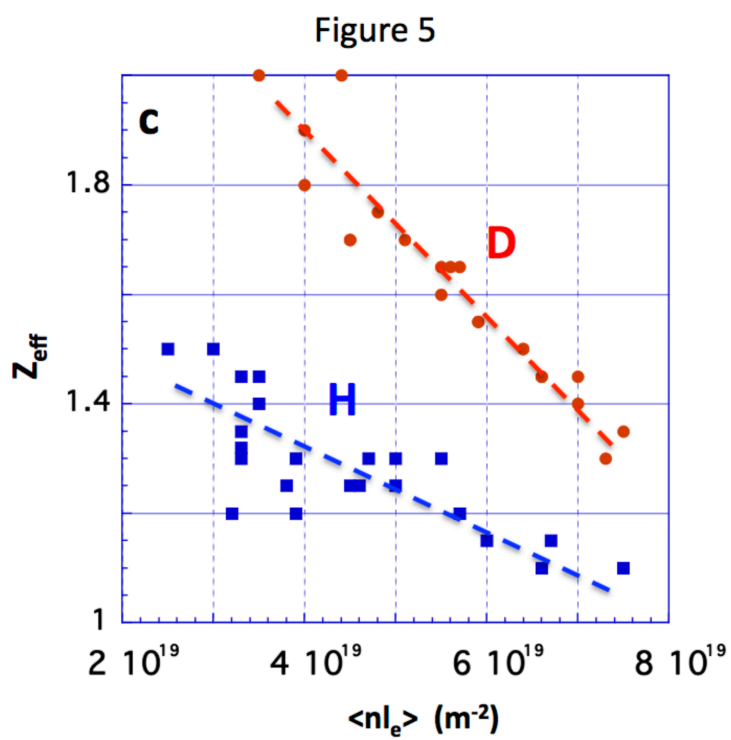


Figure 6

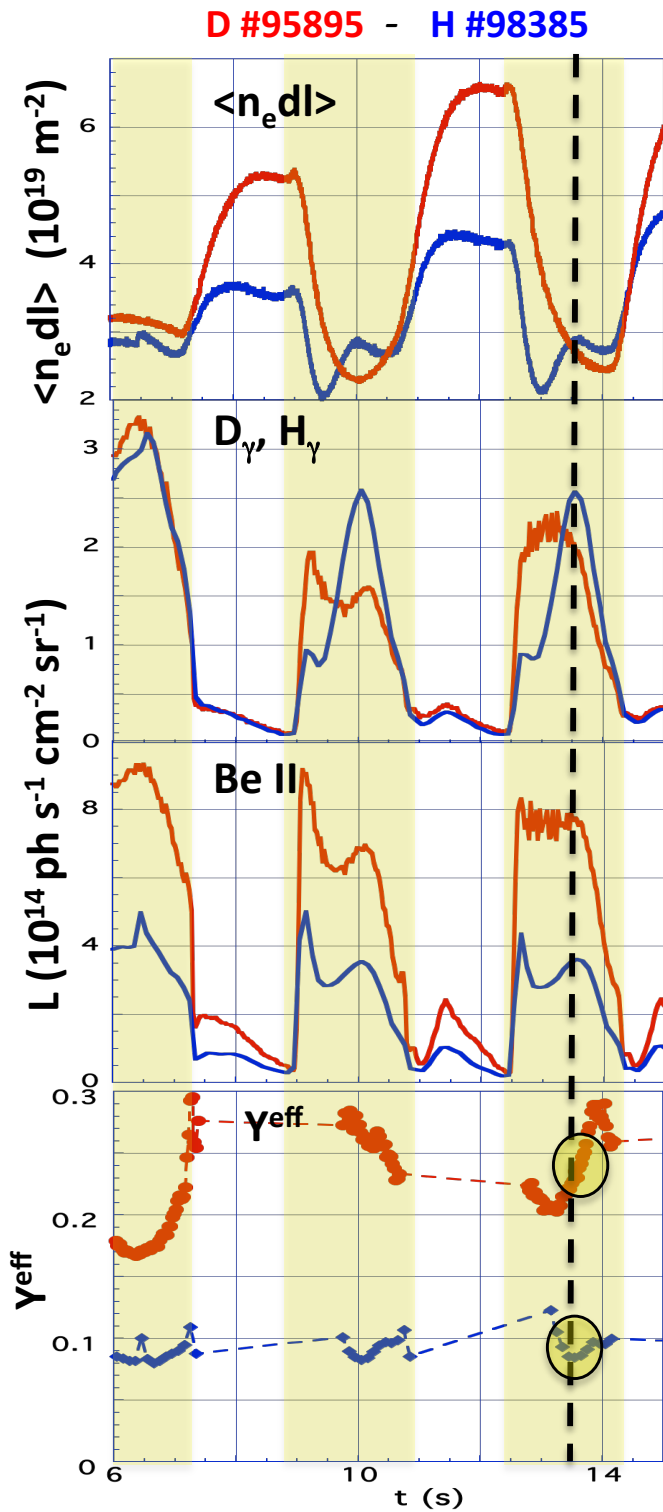


Figure 6: From top to bottom: Time traces of $\langle n_e dl \rangle$, the radiances L of the D_γ/H_γ and Be II lines and the calculated Y^{eff} for D (red) and H (blue) “limiter Cycling” plasmas. The red stripes mark the periods with the plasma leaning at the inner limiters.

Figure 7: a) Inner limiter Be II emission images at the instants marked in figure 6.
b) Outer limiter Be II emission images for other equivalent plasma pairs in in D and H.

Figure 7

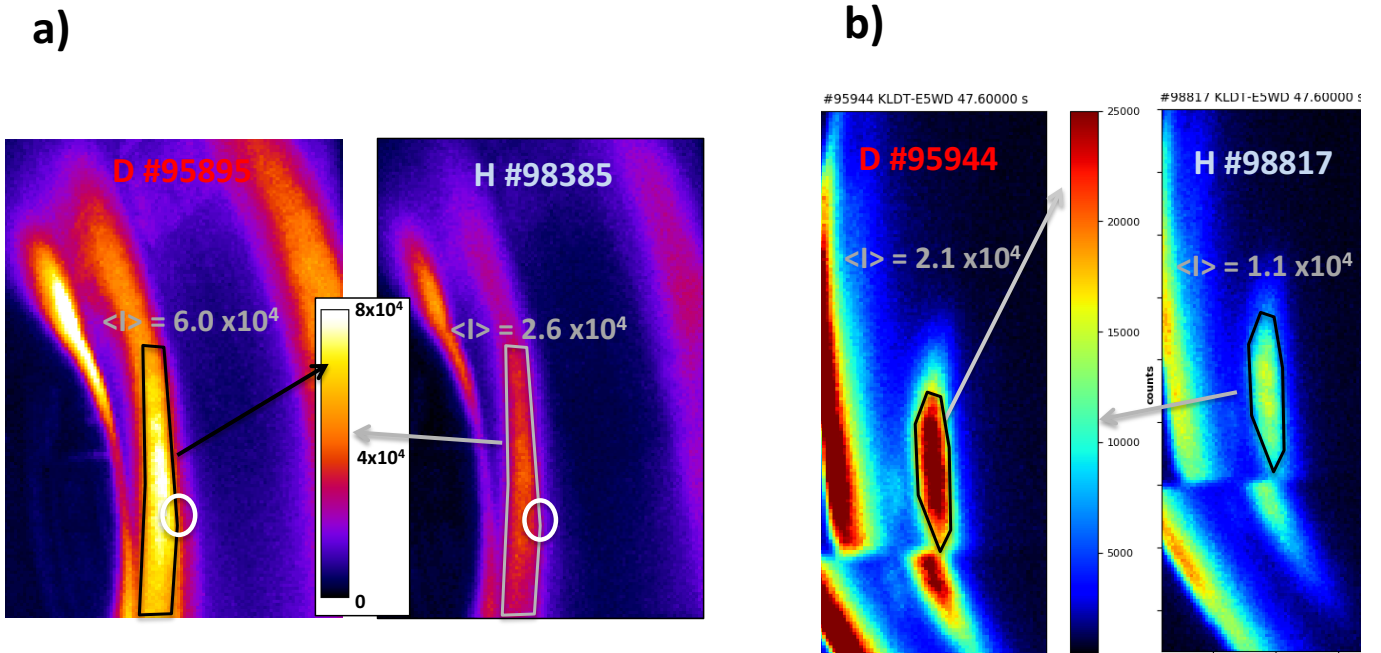


Figure 8: Calculated γ^{eff} values as a function of $\langle n l_e \rangle$ for D (red) and for H (blue) "Limiter Cycling" plasmas. The solid points are obtained from spectrometer measurements, the hollow from the cameras.

Figure 8

